How Do Annuloplasty Rings Affect Mitral Annular Strains in the Normal Beating Ovine Heart?

Wolfgang Bothe, Manuel K. Rausch, John-Peder Escobar Kvitting, Dominique K. Echtner, Mario Walther, Neil B. Ingels, Jr, Ellen Kuhl and D. Craig Miller

Circulation. 2012;126:S231-S238
doi: 10.1161/CIRCULATIONAHA.111.084046
Circulation is published by the American Heart Association, 7272 Greenville Avenue, Dallas, TX 75231

Print ISSN: 0009-7322. Online ISSN: 1524-4539

How Do Annuloplasty Rings Affect Mitral Annular Strains in the Normal Beating Ovine Heart?

Wolfgang Bothe, MD; Manuel K. Rausch, MSc; John-Peder Escobar Kvitting, MD, PhD; Dominique K. Echtner, BSc; Mario Walther, PhD; Neil B. Ingels, Jr, PhD; Ellen Kuhl, PhD; D. Craig Miller, MD

Background—We hypothesized that annuloplasty ring implantation alters mitral annular strains in a normal beating ovine heart preparation.

Methods and Results—Sheep had 16 radiopaque markers sewn equally spaced around the mitral annulus. Edwards Cosgrove partial flexible band (COS; n=12), St Jude complete rigid saddle-shaped annuloplasty ring (RSA; n=10), Carpentier-Edwards Physio (PHY; n=11), Edwards IMR ETlogix (ETL; n=11), and GeoForm (GEO; n=12) annuloplasty rings were implanted in a releasable fashion. Four-dimensional marker coordinates were obtained using biplane videofluoroscopy with the ring inserted (ring) and after ring release (control). From marker coordinates, a functional spatio-temporal representation of each annulus was generated through a best fit using 16 piecewise cubic Hermitian splines. Absolute total mitral annular ring strains were calculated from the relative change in length of the tangent vector to the annular curve as strains occurring from control to ring state at end-systole. In addition, average Green-Lagrange strains occurring from control to ring state at end-systole along the annulus were calculated. Absolute total mitral annular ring strains were smallest for COS and greatest for ETL. Strains for RSA, PHY, and GEO were similar. Except for COS in the septal mitral annular segment, all rings induced compressive strains along the entire annulus, with greatest values occurring at the lateral mitral annular segment.

Conclusions—In healthy, beating ovine hearts, annuloplasty rings (COS, RSA, PHY, ETL, and GEO) induce compressive strains that are predominate in the lateral annular region, smallest for flexible partial bands (COS) and greatest for an asymmetrical rigid ring type with intrinsic septal-lateral downsizing (ETL). However, the ring type with the most drastic intrinsic septal-lateral downsizing (GEO) introduced strains similar to physiologically shaped rings (RSA and PHY), indicating that ring effects on annular strain profiles cannot be estimated from the degree of septal-lateral downsizing. **(*Circulation*. 2012;126[suppl 1]:S231–S238.)**

Key Words: animal model ■ annulus ■ mitral regurgitation ■ mitral valve ■ strain ■ surgery

During surgical valve repair, annuloplasty devices are commonly sewn to the mitral annulus, a junctional zone between the left atrium and left ventricle (LV) that consists of a fibrous and a muscular part along the septal and lateral mitral annulus, respectively. Although the mitral annulus is a dynamic structure that undergoes considerable changes of its dimensions and its 3-dimensional (3D), saddle-like shape during the cardiac cycle,[1] the most commonly implanted annuloplasty ring type (Carpentier-Edwards Physio [PHY]) is semi-rigid and flat. As a consequence, rigid, saddle-shaped annuloplasty rings have been designed to mimic a more physiological mitral annular shape (eg, St Jude Medical RSAR [RSA]), Medtronic Profile 3D, or Carpentier-Edwards Physio II). Rings with shapes that are intentionally not physiological, however, also exist (eg, Edwards GeoForm [GEO] and IMR ETlogix [ETL]). These rings address disease-specific alterations of the mitral annulus and the left ventricle in patients with functional or ischemic mitral regurgitation, including a substantial disproportionate reduction of the septal-lateral diameter compared with the PHY ring.[2]

Recently, mitral annular strain has been measured to assess alterations in the dynamic geometry of the native mitral annulus during the cardiac cycle.[3,4] Rausch et al[4] demonstrated tensile strains along the septal part of the annulus, whereas compressive strains were observed along the lateral annular region during systole. Although it is reasonable to

From the Department of Cardiothoracic Surgery, Stanford University School of Medicine, Stanford, CA (W.B., J.P.E.K., N.B.I., E.K., D.C.M.); Department of Cardiothoracic Surgery, Friedrich Schiller University, Jena, Germany (W.B., D.K.E.); Department of Mechanical Engineering, Stanford University School of Engineering, Stanford, CA (M.K.R., E.K.); Institute of Medical Statistics, Computer Science and Documentation, Friedrich Schiller University, Jena, Germany (M.W.); Laboratory of Cardiovascular Physiology and Biophysics, Research Institute, Palo Alto Medical Foundation, Palo Alto, CA (N.B.I.).

Presented at the 2011 American Heart Association meeting in Orlando, FL, November 13–17,2011.

Correspondence to D. Craig Miller, MD, Department of Cardiothoracic Surgery, Falk Cardiovascular Research Center, Stanford University School of Medicine, Stanford, CA 94305-5247. E-mail dcm@stanford.edu

Circulation **is available at http://circ.ahajournals.org** **DOI: 10.1161/CIRCULATIONAHA.111.084046**

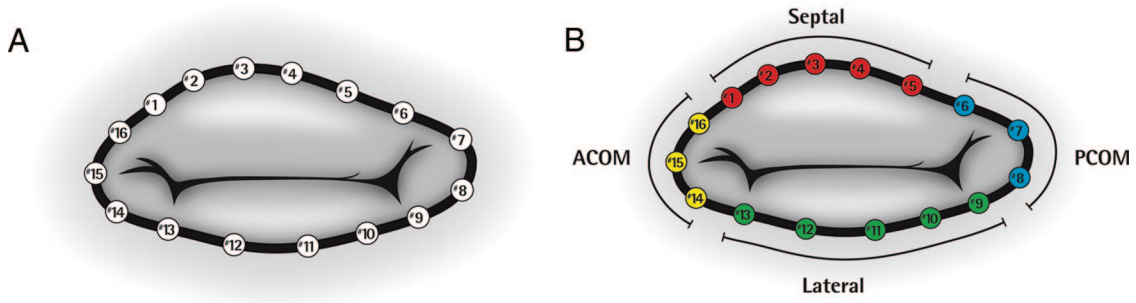

Figure 1. Array of the 16 radiopaque markers delineating the mitral annulus. Total annular average strains were calculated from all 16 annular markers (**A**) whereas regional annular strains for the septal, lateral, anterior commissure (ACOM), and posterior commissure region (PCOM) were calculated from markers 1 to 5, 9 to 13, 14 to 16, and 6 to 8, respectively (**B**). Marker 3 represents the saddle horn.

infer that the implantation of any of these described rings would alter physiological mitral annular strain patterns, the effects of different ring types on mitral annular strains have never been quantified.

Our goal was to assess the effects of 1 flexible partial band (Edwards Cosgrove [COS]) and 4 complete annuloplasty rings (RSA, PHY, ETL, and GEO) on mitral annular strains in healthy, beating ovine hearts.

Methods

All animals received humane care in compliance with the Principles of Laboratory Animal Care formulated by the National Society for Medical Research and the Guide for Care and Use of Laboratory Animals prepared by the National Academy of Sciences and published by the National Institutes of Health (DHEW [National Institutes of Health] Publication 85–23, revised 1985). This study was approved by the Stanford University Medical Center Laboratory Research Animal Review Committee and was conducted according to Stanford University policy.

Surgical Preparation

Fifty-six adult, Dorsett hybrid, male sheep (49±3kg) were premedicated with ketamine (25 mg/kg intramuscularly), anesthetized with sodium thiopental (6.8 mg/kg intravenously), intubated, and mechanically ventilated with inhalational isoflurane (1.0%–2.5%). The surgical preparation used for this dataset has been reported in detail previously.[5] In brief, a left thoracotomy was performed and the heart was suspended in a pericardial cradle. Thirteen miniature radiopaque tantalum markers were surgically implanted into the subepicardium to silhouette the LV chamber at the intersections of 2 longitudinal and 3 crosswise meridians. Using cardiopulmonary bypass and cardioplegic arrest, 16 radiopaque tantalum markers were sewn equally spaced around the mitral annulus (Figure 1A). After marker placement, 5 different annuloplasty ring models, COS, RSA, PHY, ETL, and GEO (COS, PHY, ETL, and GEO, Edwards Lifesciences, Irvine, CA; RSA, St Jude Medical Inc, St. Paul, MN) were implanted in a releasable fashion.[6] Ring and band sizes were determined by assessing the entire area of the anterior mitral leaflet using a sizer from Edwards Lifesciences (Irvine, CA). All annuloplasty devices were true-sized (because all animals had similarly sized leaflets, each received size 28 rings or bands). The animals were then transferred to the experimental catheterization laboratory for data acquisition under acute open-chest conditions.

Data Acquisition and Cardiac Cycle Timing

Videofluoroscopic images (60 Hz) of all radiopaque markers were acquired using biplane videofluoroscopy (Philips Medical Systems North America, Pleasanton, CA). First, images were acquired under baseline conditions with the ring inserted (ring). As reported, a brief period of ischemia (90 seconds) was then induced and another dataset with ring and ischemia was acquired.[7] After hemodynamics returned to normal values, the ring was released and data were acquired under baseline conditions without ring (control). Marker coordinates from 2 sinus rhythm heartbeats from both biplane views were then digitized and merged to yield the 3D coordinates of each marker centroid in each frame using semi-automated image processing and digitization software.[8] Simultaneously, analog LV pressures were recorded in real-time on the video images during data acquisition. For each beat, end-systole and end-diastole were derived from LV pressure curves as shown in Figure 2.

Absolute Total and Regional Mitral Annular Strains

From 4-dimensional marker fiduciary coordinates obtained every 16.7 ms, a functional spatio-temporal representation of each annulus was generated through a best fit using 16 piecewise cubic Hermitian splines as described.[4,9] From these smooth curves, annular strains were calculated from the local relative changes in length between 2 distinct time points for each animal and then averaged. In total, 4 sets of strains are calculated as shown in Figure 2: Strains from ed to es with ring (edR-esR) and without ring (edC-esC) are termed "cardiac cycle strains." Strains from the control state to the implanted state at ed (edR-edC) and at es (esR-esC) are termed "ring strains."

To quantify the largest cardiac cycle and ring strains in 4 different annular regions, absolute mitral annular strains were calculated individually in the septal (markers 1–5), lateral (markers 9–13), anterior commissure (markers 14–16), and posterior commissure (markers 6–8) regions as depicted in Figure 1B.

Tensile and Compressive Mitral Annular Strains

Positive strains reflecting increases in lengths or dilation are termed "tensile;" negative strains reflecting decreases in length or contraction are termed "compressive." To characterize changes in tensile and compressive strain patterns across the entire mitral annulus, average Green-Lagrange strains along the annulus were calculated for each group and projected onto an average geometric representation of their representative annuli. Note that the absolute strains described may be either tensile or compressive.

Annular Height

Because strains mainly describe alterations of the mitral annulus along the mitral annular circumference, annular height was determined to assess 3D geometry of the mitral valve annulus with and without annuloplasty ring. Annular height was referenced to the best-fit plane through the spatio-temporal representation of each annulus and defined as the orthogonal distance from each point along the annulus to this plane.

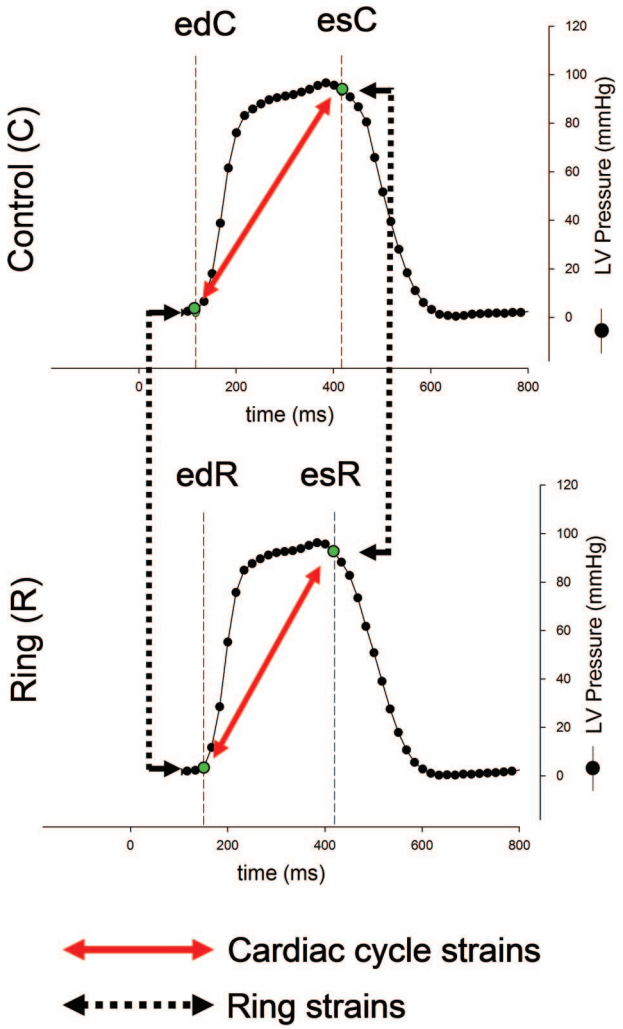

Figure 2. Schematic illustrating cardiac cycle timing and the calculation of cardiac cycle and ring strains. The 2 curves represent left ventricular (LV) pressure curves from 1 representative animal with ring (RING) and without ring (CONTROL). End diastole (ed) and end systole (es) were derived from LV pressure curves as shown. Cardiac cycle strains were defined as strains from ed to es either with ring (RING, lower red solid arrow) or without ring (CONTROL, upper red solid arrow). Ring strains describe strains occurring on ring implantation at ed (left black dotted arrow) or es (right black dotted arrow; see Methods for details).

Statistical Analysis

Average values of all animals in the respective groups were reported as mean±1 SD. Hemodynamic data with and without annuloplasty ring (or band) were compared using 1-way repeated-measures ANOVA with a Holm-Sidak post hoc test (Sigmaplot 11.0; Systat Software, San Jose, CA). Mitral annular strain data were statistically evaluated by comparing cardiac cycle strains with and without annuloplasty ring (edC-esC vs edR-esR). Similarly, ring strains were compared at end-diastole and end-systole (edR-edC vs esR-esC). Furthermore, differences between ring types (COS vs RSA vs PHY vs ETL vs GEO) were assessed. We applied linear mixed models including an interaction term between strains and ring types. We used unstructured covariance pattern to account for different variances and correlation between strains. A $P<0.05$ was considered statistically significant. To adjust for multiplicity, we applied Holm sequential Bonferroni method for pair-wise comparison. Statistical strain analyses were performed using SAS 9.3 SAS Institute Inc., Cary, NC).

Results

Hemodynamics

The Table shows selected hemodynamic variables, including heart rate, LV end-diastolic volume, and maximum left ventricular dP/dt. Except for COS, in which maximum dP/dt was slightly higher compared with control, no relevant differences were found between ring and control states in all 5 groups.

Absolute Total Cardiac Cycle and Ring Strains

Figures 3A and 3B depict absolute total cardiac cycle and ring strains, respectively. Total cardiac cycle strains with ring were significantly smaller than without ring (edR-esR vs. edC-esC, Figure 3A) for all rings. Total annular ring strains (edR-edC and esR-esC, Figure 3B) were greater than cardiac cycle strains with no ring implanted (edC-esC, Figure 3A) and smallest for COS and greatest for ETL. Total annular ring strains for GEO were similar to RSA and PHY. There was a tendency for total mitral annular ring strains to be greater at end-diastole than end-systole (edR-edC vs esR-esC, Figure 3B) for all rings (but this was only statistically significant for ETL and GEO).

Absolute Regional Cardiac Cycle and Ring Strains

Figure 4A–H shows absolute cardiac cycle and ring strains in the septal (Figure 4A, B), lateral (Figure 4C, D), anterior commissure (Figure 4E, F) and posterior commissure (Figure 4G, H) regions of the mitral annulus. In the septal annular region, representing the fibrous part of the annulus, ring strains (edR-edC and esR-esC) were greater with RSA, PHY, ETL, and GEO compared with cardiac cycle strains in the control state (edC-esC), whereas ring strains with COS were similar to cardiac cycle strains without ring in this annular region (Figure 4A, B).

In the lateral region, cardiac cycle strains in the control state (edC-esC) were significantly greater than cardiac cycle strains with ring implanted (edR-esR) in all ring groups (COS, RSA, PHY, ETL and GEO, edR-esR; Figure 4C). Ring strains (edR-edC and esR-esC) in the lateral annular region were greater with all rings (COS, RSA, PHY, ETL, and GEO) compared with cardiac cycle strains in the control state (edC-esC; Figure 4C, D).

There was a trend that ring strains (edR-edC and esR-esC) were greatest for ETL compared with the other ring types in all regions of the mitral annulus (septal, lateral, anterior commissure, and posterior commissure, Figure 4B, D, F, H). GEO, the ring that includes a nonphysiological elevation of the lateral ring segment, had strain profiles in this annular portion that were similar to COS, RSA, and PHY.

Tensile and Compressive Cardiac Cycle and Ring Strains

Figure 5 shows color maps of average tensile and compressive cardiac cycle and ring strains. Whereas cardiac cycle strains in the control state (edC-esC) were tensile in all groups in the septal region, compressive cardiac cycle strains without ring were observed in the lateral region. Cardiac cycle strains with ring implanted (edR-esR) were minimal along the entire annulus with any of the rings implanted (COS, RSA, PHY,

Table. Hemodynamics

	HR (min^{-1})	*P* vs CTRL	LVEDV (mL)	*P* vs CTRL	dP/dt_{max} (mm Hg)	*P* vs CTRL
COS-CTRL	98±14		120±15		1360±317	
COS	98±13	0.91	121±16	.392	1527±386	0.001
RSA-CTRL	85±16		120±24		1309±444	
RSA	85±13	0.73	120±21	.810	1232±324	0.28
PHY-CTRL	93±11		123±22		1350±313	
PHY	93±10	0.76	123±24	.854	1395±311	0.52
ETL-CTRL	82±6		125±20		1169±368	
ETL	80±9	0.53	125±20	.833	1190±363	0.26
GEO-CTRL	92±10		114±13		1313±315	
GEO	93±10	0.49	113±13	.223	1388±41	0.070

COS indicates Edwards Cosgrove band; CTRL, control; dP/dt_{max}, maximum dP/dt; ETL, Edwards IMR ETlogix; GEO, Edwards GeoForm; LVEDV, left ventricular end-diastolic volume; PHY, Carpentier-Edwards Physio; RSAR, St Jude Medical rigid saddle-shape annuloplasty ring; SD, standard deviation.

All values are mean±1 SD.

ETL, and GEO) except for the septal region with COS, where tensile strain patterns similar to those during the control state were observed. Except for the septal region of COS, ring strains (edR-edC and esR-esC) were compressive along the entire annulus with all rings (COS, RSA, PHY, ETL, and GEO) and with highest values occurring in the lateral annular region.

Annular Height

Figure 6 shows color maps of annular height. Compared with the control state, COS and RSA have negligible effects on annular height whereas PHY and ETL reduce annular height, especially in the septal (ie, saddle horn [marker 3]) annular region. GEO reduces annular height in the saddle horn region, but an increase in annular height is observed in the lateral annular region.

Discussion

The principal findings of this study were: (1) absolute total ring strains were greater with all rings than cardiac cycle strains in the control state; (2) absolute total ring strains were smallest for COS and greatest for ETL, whereas they were similar for GEO, RSA, and PHY; (3) except for the septal region with COS, ring strains were compressive along the entire annulus with all rings, with highest values occurring in the lateral annular region; and (4) PHY and ETL reduced annular height in the septal and the lateral annular segment, but COS and RSA did not. GEO reduced annular height in the septal region but increased annular height in the lateral annular region.

Mitral annular ring strains, ie, strains occurring on the implantation of an annuloplasty ring, have never been described or quantified previously. Expectedly, the COS, a flexible, partial band that spares the septal portion of the mitral annulus, induced negligible ring strains to the septal mitral annular region. Furthermore, tensile systolic strain patterns similar to those during the control state and no changes in annular height profiles were observed in this annular segment. The maintenance of physiological mitral annular dimensions, dynamics, and shape in the septal annular portion could, in part, explain our recent finding that the COS, unlike complete, rigid rings, did not alter anterior mitral leaflet strains.[5] Furthermore, the observed preservation of annular height profiles could help to provide a maximum amount of leaflet coaptation as suggested by Vergnat et al[10] and Jensen et al.[11] To our surprise, the COS imposed significant ring strains to the lateral annular portion in an amount that was similar to RSA and PHY. Because mitral annular strain is a parameter that reflects alterations in the circumference of the mitral annulus, we speculate that the length of the COS is similar to the circumference of the lateral portion of RSA and PHY.

The finding that ring strain patterns observed with RSA and PHY were similar may be attributed to the fact that both rings have similar dimensions;[2] however, unlike RSA, which preserved the physiological 3D profile of the mitral annulus,

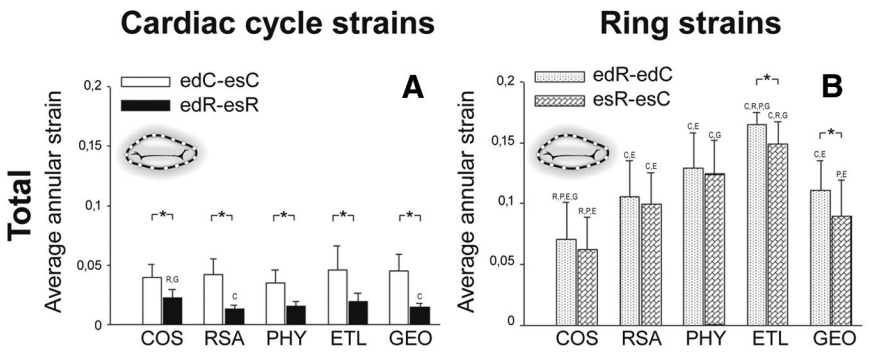

Figure 3. Absolute total average mitral annular cardiac cycle (**A**) and ring strains (**B**). Note that absolute strains are characterized by positive values only and, thus, do not reflect lengthening or shortening (see Methods for details). COS indicates Edwards Cosgrove band; RSAR, St Jude Medical rigid saddle-shape annuloplasty ring; PHY, Carpentier-Edwards Physio; ETL, Edwards IMR ETlogix; GEO, Edwards GeoForm. C, R, P, E, and G: $P<0.05$ vs COS, RSA, PHY, ETL, and GEO, respectively. *$P<0.05$. ed indicates end diastole; es, end systole; C, control, R, ring.

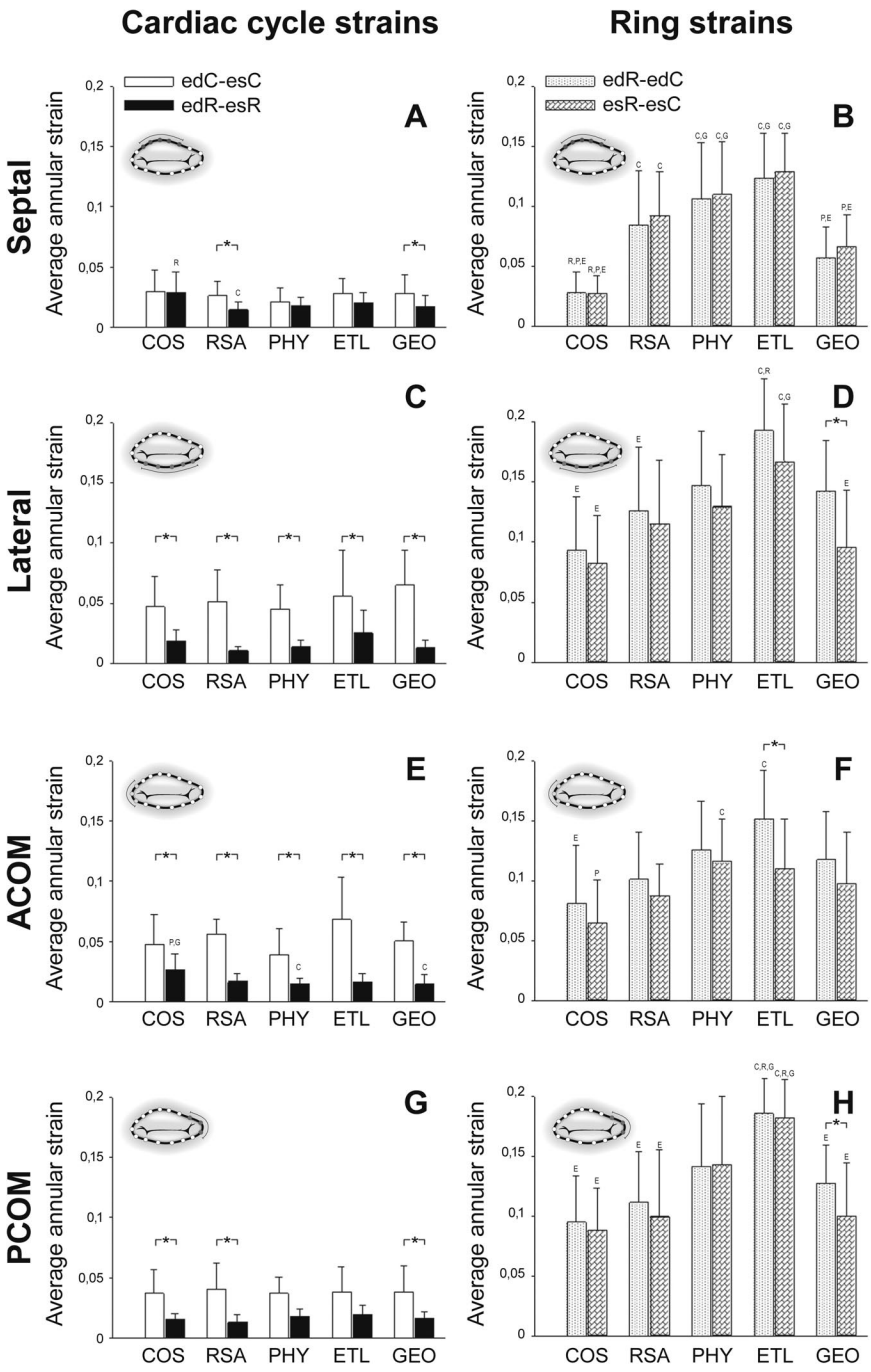

Figure 4. Absolute regional cardiac cycle (**A**, **C**, **E**, **G**) and ring strains (**B**, **D**, **F**, **H**) for the septal (**A**, **B**), lateral (**C**, **D**), anterior commissure (ACOM) (**E**, **F**), and posterior commissure region (PCOM) (**G**, **H**) of the annulus. Note that absolute strains are characterized by positive values only and, thus, do not reflect lengthening or shortening (see Methods for details). COS indicates Edwards Cosgrove band; RSAR, St Jude Medical rigid saddle-shape annuloplasty ring; PHY, Carpentier-Edwards Physio; ETL, Edwards IMR ETlogix; GEO, Edwards GeoForm. C, R, P, E, and G: $P<0.05$ vs COS, RSA, PHY, ETL, and GEO, respectively. *$P<0.05$. ed indicates end diastole; es, end systole; C, control; R, ring.

the PHY ring reduced annular height. This reduction in annular height predominantly occurred in the septal annular segment, a finding that may be attributed to the fact that the septal part includes the highest segment (in the natural mitral annulus) with the greatest distance to the annular plane. Consequently, it is expected that the most drastic effects occur in this mitral annular portion. However, although the PHY ring had the greatest effects on the mitral annular 3D profile in the septal annular region, the ring introduced the greatest strains to the lateral annular segment, indicating that changes in mitral annular strain patterns are not in direct proportion to alterations in the 3D mitral annular profile. These findings reflect the complexity of the changes that are introduced to the mitral annulus on the implantation of an annuloplasty ring and should be considered when a mitral repair is performed.

The ETL ring is specifically designed for the treatment of patients with ischemic mitral regurgitation and includes a disproportionate reduction of ≈10% of the septal-lateral diameter compared with the PHY ring.[2] In addition, the design of the ring is slightly asymmetrical with a pronounced reduction of the region subtending the posteromedial mitral leaflet scallop and posterior commissure.[12] The ETL imposed the greatest ring strains on all regions of all rings. As discussed, strain is a parameter that is most sensitive to changes in annular circumference. It therefore may be as-

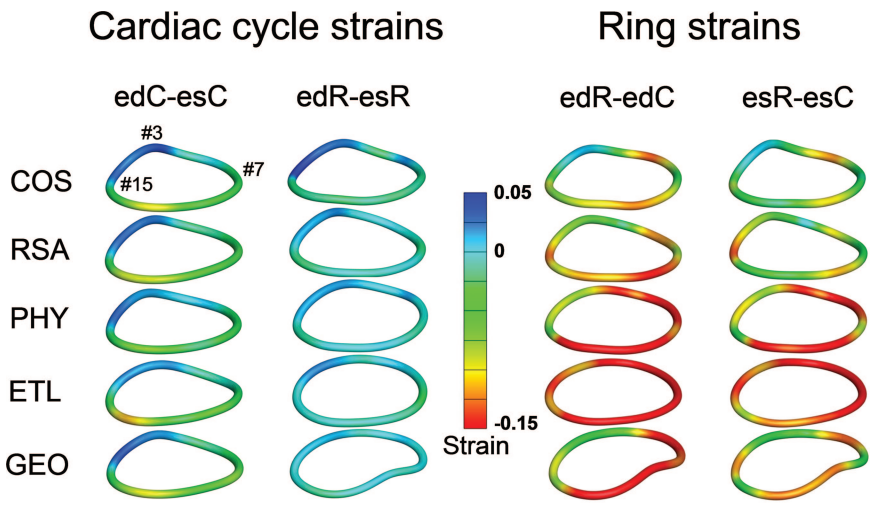

Figure 5. Color maps of average tensile and compressive cardiac cycle and ring strains. COS indicates Edwards Cosgrove band; RSAR, St Jude Medical rigid saddle-shape annuloplasty ring; PHY, Carpentier-Edwards Physio; ETL, Edwards IMR ETlogix; GEO, Edwards GeoForm. Markers 3, 7, and 15 represent saddle horn, posterior commissure, and anterior commissure, respectively (see Figure 1). ed indicates end diastole; es, end systole; C, control; R, ring.

sumed that the ETL has the smallest circumference of all rings, resulting in the greatest ring strains.

Surprisingly, the GEO, which includes the most radical disproportionate reduction of the septal-lateral diameter of all rings (≈25%), did not impose the greatest ring strains compared with the other ring types. Because it is has been demonstrated that the GEO has a greater diameter in the anterior commissure–posterior commissure diameter than ETL,[2,13] it is presumed that GEO has a greater circumference, which, in turn, may explain why it induces less ring strains than the ETL. These findings indicate that ring effects on annular strain profiles cannot be estimated by the degree of septal-lateral downsizing. Another feature of the GEO is the elevation of the midlateral annular segment. This ring characteristic has been associated with ring dehiscences clinically.[14] Interestingly, average annular strains in this area were similar to those of COS, RSA, and PHY. It therefore is reasonable to speculate that the observed ring dehiscences may be attributed more to the alterations in the 3D annular profile (an increase in annular height in this region; Figure 6) than to an increase in mitral annular strains.

Mitral Annular Strains: What Are We Measuring?

Recent engineering studies have focused on characterizing annular strains to provide insight into temporal and regional variations of annular contraction and dilation. Cardiac cycle strains without ring (edC-esC) are a measure of how much the native annulus contracts and dilates throughout the cardiac cycle. The cardiac cycle strains reported in this article are in excellent qualitative and quantitative agreement with the natural annular strains reported by Eckert et al[3] and Rausch et al.[9] Cardiac cycle strains with ring (edR-esR) are a measure of how much the annulus with ring contracts and dilates throughout the cardiac cycle. The cardiac cycle strains with rings reported in this article are in agreement with previously published data.[4] Figure 5 (column 2) confirms the general intuition that stiffer rings (RSA, PHY, ETL, and GEO) constrain annular dynamics more than flexible annuloplasty bands (COS). Ring strains at end-diastole and end-systole (ie, edC-edR and esC-esR) are measures of how much annuloplasty devices constrain the circumference of the native mitral annulus. Ring strains have never been reported to date. Only the combination of permanent implantable markers and the releasable ring technique allows us to quantify ring induced strains. Here, we restrict ourselves to report kinematic measurements, ie, displacements and strain, which are directly extracted from our raw data. These data are not a direct measure of force. Reporting forces would require assumptions that might induce errors. Although no force measurements are provided, regional strain maps as shown in Figure 5 provide mechanistic insight into the functionality of

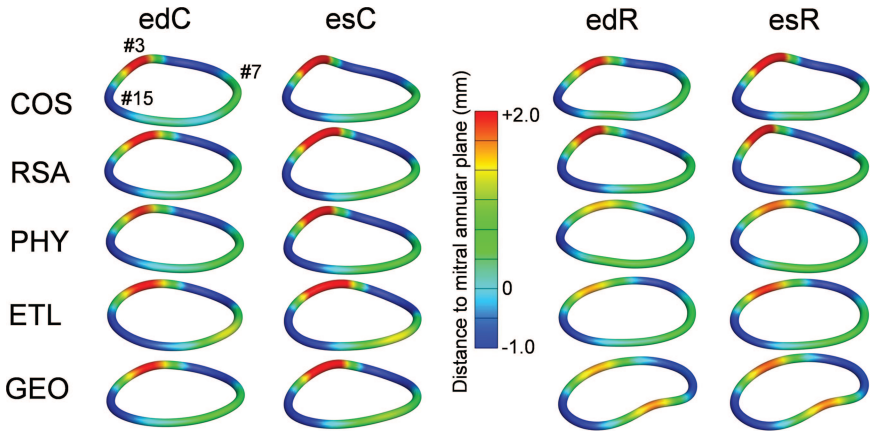

Figure 6. Color maps of annular height represented by the distance of each annular segment to a best-fit mitral annular plane. COS indicates Edwards Cosgrove band; RSAR, St Jude Medical rigid saddle-shape annuloplasty ring; PHY, Carpentier-Edwards Physio; ETL, Edwards IMR ETlogix; GEO, Edwards GeoForm. Markers 3, 7, and 15 represent saddle horn, posterior commissure, and anterior commissure, respectively (see Figure 1). ed indicates end diastole; es, end systole; C, control; R, ring.

different annuloplasty rings and may help the rational design of more physiological devices with improved long-term durability.

Clinical Inferences

Despite successful mitral repair with annuloplasty ring implantation, recurrent mitral regurgitation may occur in ≈5% to 10% of patients with organic mitral valve disease[15] and upwards of 30% or more of patients with functional/ischemic mitral regurgitation.[16,17] A potential device-related cause for recurrent mitral valve regurgitation includes ring dehiscence.[18–20] It is logical to think that major perturbations of physiological annular strain patterns and/or 3D annular profiles—as our findings demonstrated—increase the risk for ring dehiscence. It is, however, of note that an increased risk for a postoperative ring dehiscence also may be present if mitral annular strain profiles after ring implantation are normal. Such an increased risk for dehiscence may be attributable to a nonphysiological 3D ring profile such as the lateral portion of the GEO.

Another contributing factor to suboptimal outcomes after surgical mitral valve repair may be the fact that several steps during a repair such as ring type or size selection are currently more so based on surgical expertise and intuition than on quantitative data. To date, no studies exist comparing the effects of different ring types on mitral annular strains. Furthermore, the dimensions of mitral annuloplasty rings are not fully provided by manufacturers. This lack of provision may be attributable to commercial reasons or simply because of practical difficulties in measurements. With the introduction of complexly shaped 3D rings, it has become difficult to provide a reasonable circumference for a given annuloplasty ring. Consequently, it is almost impossible for a surgeon to estimate the effects of an annuloplasty ring on mitral annular strain patterns. The quantitative and qualitative annular strain data with and without annuloplasty rings as well as the 3D mitral annular profiles reported in this study not only may provide mechanistic insight into the functionality of different annuloplasty rings but also may help to guide more rational planning and conduction of surgical mitral valve repair and to potentially improve the designs of current annuloplasty rings and, ultimately, patient outcomes.

Study Limitations

Limitations inherent to this experimental model using normal sheep hearts have been addressed in detail previously.[5] Annuloplasty rings are implanted in patients with mitral regurgitation undergoing surgical valve repair to restore mitral annular dimensions that allow a sufficient amount of leaflet coaptation and to stabilize the repair. Typically, in patients with structural or ischemic/functional mitral regurgitation, a large degree of mitral annular dilatation is present, which is not seen in this healthy heart preparation. It is reasonable to speculate, however, that the changes in strain patterns observed after ring implantation in healthy hearts might be even more pronounced when mitral annular dilatation is present. This notion is supported by the finding that there was a tendency that ring strains were greatest at end-diastole, a time point in the cardiac cycle when the mitral annulus has its largest dimensions.

Conclusions

In healthy, beating ovine hearts, annuloplasty rings (COS, RSA, PHY, ETL, and GEO) induce compressive ring strains that are: (1) greater than cardiac cycle strains without ring; (2) predominate in the lateral annular region; and (3) smallest for flexible partial bands (COS) and greatest for an asymmetrical rigid ring type with intrinsic septal-lateral downsizing (ETL). However, the ring type with the most drastic intrinsic septal-lateral downsizing (GEO) introduced strains that were similar to those induced by physiologically shaped rings (RSA and PHY), indicating that ring effects on annular strain profiles cannot be estimated from the degree of septal-lateral downsizing. Clinical investigation is necessary to determine whether annuloplasty rings affect annular strain patterns in humans and whether any such potential perturbation adversely influences clinical outcomes.

Acknowledgments

The authors gratefully acknowledge the expert technical assistance of Carolin Berg, Maggie Brophy, Sigurd Hartnett, Saideh Fahramandnia, and George T. Daughters II.

Sources of Funding

D.C.M. received R01 research grant from NHLBI, National Institutes of Health HL29589 (1982–2008) and R01 research grant from NHLBI, National Institutes of Health HL67025 (2001–2010). E.K. received NSF CAREER Award CMMI-0952021. J.P.E.K. received funding from the US–Norway Fulbright Foundation, the Swedish Heart-Lung Foundation, and the Swedish Society for Medical Research.

Disclosures

D.C.M. is a consultant for Medtronic CardioVascular Division.

References

1. Timek TA, Miller DC. Experimental and clinical assessment of mitral annular area and dynamics: what are we actually measuring? *Ann Thorac Surg*. 2001;72:966–974.
2. Bothe W, Swanson JC, Ingels NB, Miller DC. How much septal-lateral mitral annular reduction do you get with new ischemic/functional mitral regurgitation annuloplasty rings? *J Thorac Cardiovasc Surg*. 2010;140:117–121, 121e1–121e3.
3. Eckert CE, Zubiate B, Vergnat M, Gorman JH III, Gorman RC, Sacks MS. In vivo dynamic deformation of the mitral valve annulus. *Ann Biomed Eng*. 2009;37:1757–1771.
4. Rausch MK, Bothe W, Kvitting JP, Swanson JC, Miller DC, Kuhl E. Mitral valve annuloplasty: a quantitative clinical and mechanical comparison of different annuloplasty devices. *Ann Biomed Eng*. 2012;40:750–761.
5. Bothe W, Kuhl E, Kvitting JP, Rausch MK, Goktepe S, Swanson JC, Farahmandnia S, Ingels NB Jr, Miller DC. Rigid, complete annuloplasty rings increase anterior mitral leaflet strains in the normal beating ovine heart. *Circulation*. 2011;124:S81–S96.
6. Bothe W, Chang PA, Swanson JC, Itoh A, Arata K, Ingels NB, Miller DC. Releasable annuloplasty ring insertion–a novel experimental implantation model. *Eur J Cardiothorac Surg*. 2009;36:830–832.
7. Bothe W, Kvitting JP, Stephens EH, Swanson JC, Liang DH, Ingels NB Jr, Miller DC. Effects of different annuloplasty ring types on mitral leaflet tenting area during acute myocardial ischemia. *J Thorac Cardiovasc Surg*. 2011;141:345–353.
8. Niczyporuk MA, Miller DC. Automatic tracking and digitization of multiple radiopaque myocardial markers. *Comput Biomed Res*. 1991;24:129–142.

9. Rausch MK, Bothe W, Kvitting JP, Swanson JC, Ingels NB Jr, Miller DC, Kuhl E. Characterization of mitral valve annular dynamics in the beating heart. *Ann Biomed Eng*. 2011;39:1690–1702.
10. Vergnat M, Jackson BM, Cheung AT, Weiss SJ, Ratcliffe SJ, Gillespie MJ, Woo YJ, Bavaria JE, Acker MA, Gorman RC, Gorman JH III Saddle-shape annuloplasty increases mitral leaflet coaptation after repair for flail posterior leaflet. *Ann Thorac Surg*. 2011;92:797–803.
11. Jensen MO, Jensen H, Levine RA, Yoganathan AP, Andersen NT, Nygaard H, Hasenkam JM, Nielsen SL. Saddle-shaped mitral valve annuloplasty rings improve leaflet coaptation geometry. *J Thorac Cardiovasc Surg*. 2011;142:697–703.
12. Daimon M, Fukuda S, Adams DH, McCarthy PM, Gillinov AM, Carpentier A, Filsoufi F, Abascal VM, Rigolin VH, Salzberg S, Huskin A, Langenfeld M, Shiota T. Mitral valve repair with Carpentier-McCarthy-Adams IMR ETlogix annuloplasty ring for ischemic mitral regurgitation: early echocardiographic results from a multi-center study. *Circulation*. 2006;114:I588—I593.
13. Bothe W, Kvitting JP, Swanson JC, Hartnett S, Ingels NB Jr, Miller DC. Effects of different annuloplasty rings on anterior mitral leaflet dimensions. *J Thorac Cardiovasc Surg*. 2010;139:1114–1122.
14. De Bonis M, Taramasso M, Grimaldi A, Maisano F, Calabrese MC, Verzini A, Ferrara D, Alfieri O. The GeoForm annuloplasty ring for the surgical treatment of functional mitral regurgitation in advanced dilated cardiomyopathy. *Eur J Cardiothorac Surg*. 2011;40:488–495.
15. Mohty D, Orszulak TA, Schaff HV, Avierinos JF, Tajik JA, Enriquez-Sarano M. Very long-term survival and durability of mitral valve repair for mitral valve prolapse. *Circulation*. 2001;104:I1–I7.
16. Shiota M, Gillinov AM, Takasaki K, Fukuda S, Shiota T. Recurrent mitral regurgitation late after annuloplasty for ischemic mitral regurgitation. *Echocardiography*. 2011;28:161–166.
17. Tahta SA, Oury JH, Maxwell JM, Hiro SP, Duran CM. Outcome after mitral valve repair for functional ischemic mitral regurgitation. *J Heart Valve Dis*. 2002;11:11–18, discussion 18–9.
18. Shimokawa T, Kasegawa H, Katayama Y, Matsuyama S, Manabe S, Tabata M, Fukui T, Takanashi S. Mechanisms of recurrent regurgitation after valve repair for prolapsed mitral valve disease. *Ann Thorac Surg*. 2011;91:1433–1438, discussion 1438–9.
19. Tsang W, Wu G, Rozenberg D, Mosko J, Leong-Poi H. Early mitral annuloplasty ring dehiscence with migration to the descending aorta. *J Am Coll Cardiol*. 2009;54:1629.
20. Kronzon I, Sugeng L, Perk G, Hirsh D, Weinert L, Garcia Fernandez MA, Lang RM. Real-time 3-dimensional transesophageal echocardiography in the evaluation of post-operative mitral annuloplasty ring and prosthetic valve dehiscence. *J Am Coll Cardiol*. 2009;53:1543–1547.